JOURNAL OF THERMOPHYSICS AND HEAT TRANSFER
Vol. 7, No. 4, Oct.–Dec. 1993

Surface Temperature Measurement in Semitransparent Media

F. Z. Roissac,* T. T. Osman,† and J. F. Sacadura‡
Institut National des Sciences Appliquées de Lyon, 69621 Villeurbanne, France

The surface temperature of a semitransparent wall, placed in a convective medium and exposed to external radiation (e.g., building window glasses) can be well approached using a remote sensing technique associated with a correction model. Radiometric measurement is first carried out on an opaque small size black target, which is glued on the concerned surface. This measurement can then be corrected to get the "real" temperature through a model solving a combined conduction-radiation heat transfer problem.

Nomenclature

A = thermocouple wire surface area, m^2
B = Biot number, Eqs. (2)
D = reduced variable, Eqs. (2)
F = blackbody emissive power fraction
G = heat generation (source) term, Eqs. (1) and (2)
H = global heat transfer coefficient, $W \cdot m^{-2} \cdot K^{-1}$
I = exernal radiative flux incident on the surface, $W \cdot m^{-2}$
J = Bessel function of the first kind
k = thermal conductivity, $W \cdot m^{-1} \cdot K^{-1}$
Q = radiative heat flux, $W \cdot m^{-2}$
R = dimensionless radial distance, dimensionless radius
r = radial distance, radius, m
T = temperature, K or °C
Z = dimensionless axial distance
z = axial distance, m
α = absorptivity (target and thermocouples)
β = eigenvalue
γ = radiation propagation angle, measured from the normal to the surface
ΔT = temperature correction, K or °C
ε = emissivity
θ = reduced temperature
κ = volumetric spectral absorption coefficient, m^{-1}
λ = wavelength, μm
μ = cos γ
ρ = spectral reflectivity
σ = Stefan-Boltzmann constant
τ = spectral transmissivity

Subscripts
c = collimated, or thermocouple property
d = diffuse
e = exterior
i = interior
l = relative to the limit angle of refraction
m = relative to the mth eigenvalue
n = relative to the nth spectral band $n \in (1, N)$
p = relative to the pth zone created by the target $p \in (1, M)$, Fig. 2
t = target
w = wall
$z1$ = first thermocouple position
$z2$ = second thermocouple position

Superscripts
a = ambient
s = surface
~ = integral transform of a variable

Received March 24, 1992; revision received Oct. 28, 1992; accepted for publication Oct. 29, 1992.

*Doctoral Student, Centre de Thermique—URA CNRS 1372; currently Research Engineer, Renault Véhicules Industriels, 69800 Saint Priest, France.

†Teaching and Research Fellow, Centre de Thermique—URA CNRS 1372; currently Maître de Conférences, IUT d'Orsay, Université Paris XI, France.

‡Professor, CETHIL, Centre de Thermique—URA CNRS 1372.

Introduction

SURFACE temperature measurement is a difficult metrological problem, particularly when dealing with semitransparent materials. These materials are widely used in buildings, means of transportation, solar energy installations, spacecraft, and many other thermal systems. In such systems, it is often necessary to know the surface temperature of these materials to compute the heat exchange with the surroundings. Several errors may arise in either contact or remote measuring methods. If contact thermometric sensors are used, even if their size is small, they perturb the temperature field and interact with the surrounding thermal conditions.[1,2] On the other hand, the use of pyrometric devices leads to erroneous surface temperature measurements due to the semitransparent character of such materials, the influence of reflected radiation, and also to the use of inaccurate radiative properties data.[2,3]

The work presented in this article is part of a research program devoted to the assessment of different methods for surface temperature measurement of building window glasses exposed to solar irradiation. The object was to develop methods that could be used for the validation of building energy consumption and thermal comfort computations.

Several contact and noncontact measurement techniques were studied in this program. The present work deals with the infrared (IR) pyrometric techniques. The main advantages of these over thermocouples and other contact sensors are the ease of use for outdoor controls (fine wire thermocouples are generally too fragile) and absence of errors due to contact resistance problems. So IR pyrometers are frequently used in building thermal controls. But other uncertainties arise from radiation measurements. A method to decrease the errors inherent to such pyrometric measurements is presented here.

This method is based on radiometric measurements carried out on a very thin opaque spot (target) of well-known spectral radiative properties, and perfectly adhered to the semitransparent wall. In this method, the influence of subsurface radiation is eliminated. The corresponding surface temperature is still inaccurate, mainly due to perturbations of the temperature field created by the target. Consequently, it is necessary to quantify these perturbations in order to obtain the "true" temperature. The perturbations were estimated through

a coupled conduction-radiation heat transfer model, developed here to compute the temperature field in a semitransparent slab, taking into account the target effect and the various external conditions. The difference between the target center temperature and the temperature at a surface point sufficiently far from it, closely approaches the introduced perturbation. The "exact" surface temperature may then be obtained by adding the quantified perturbation to the measured temperature.

In order to test the feasibility of this method, an experimental setup was built allowing the simultaneous measurement of the surface temperature of a semitransparent plate by two different methods: 1) the radiometric one under test, and 2) from thermocouples embedded in the sample.

Due to the difficulty of embedding thermocouples in a glass plate, after some unsuccessful attempts made by a glass manufacturer, Plexiglas® was selected.

By extrapolation of the thermocouple measurements, very accurate surface temperature data are obtained, which are taken as a reference for the comparison with the radiometric results.

The model used to correct the pyrometric measurements is presented first. A numerical exploration of this model is then briefly reported, as well as the model allowing to extrapolate the surface temperature from temperatures measured inside the material. Finally, the results obtained from experiments performed in a controlled cell and in outdoor ambiances are presented and discussed.

Measurement Correction Model

The problem may be stated as follows: a semitransparent wall of large radius-to-thickness ratio (r_w/z_{max}) separates an "external" from an "internal" media. This is the case, e.g., of a window glass. κ, k, and the spectral refractive index of the semitransparent wall are assumed known. The ambient temperature and global heat transfer coefficient on both external and internal sides are T_e^a, H_e and T_i^a, H_i, respectively. The external surface is exposed to diffuse isotropic and/or collimated radiation of intensity I_d and I_c, respectively. The external surface temperature of the slab is sought.

To find the external surface temperature, a very thin opaque target of radius r_t and spectral absorptivity α_t is perfectly glued to the external surface. Temperature measurements are carried out using an IR radiometer viewing the target. This measurement does not yield the correct surface temperature due to the perturbation introduced by the target to the real temperature field. In addition, the target reflects a part of the incident radiation towards the pyrometer causing another error. This later difficulty may be overcome by selecting a target of low reflectivity, as will be shown later. We shall first deal with the perturbation introduced by the target. The measured temperature may be corrected by adding a correction term obtained from the solution of the problem represented on Fig. 1.

The analysis is carried out under the following assumptions: 1) steady-state, axisymmetry, and constant thermal properties; 2) the material is homogeneous, isotropic, and scattering is negligible; 3) the interfaces are optically smooth, and plane parallel to each other; 4) the thickness of the layer is much greater than the radiation wavelength so that optical interference effects can be neglected; 5) the temperature of the medium is sufficiently low so that internal emission can be neglected compared to the absorption of external radiation (cold medium assumption); and 6) the radiation field incident onto the layer is resolved into a collimated and diffuse component. The mathematical model is briefly described below:

$$\frac{1}{R}\frac{\partial}{\partial R}\left[R\frac{\partial\theta(R,Z)}{\partial R}\right]+\frac{\partial^2\theta(R,Z)}{\partial Z^2}+G=0 \qquad 0<R<1,\quad 0<Z<Z_{max}$$

$$-\frac{\partial\theta(R,Z)}{\partial Z}+B_e\cdot\theta(R,Z)=\begin{cases}B_e\cdot\theta_e^a+D & 0<R<R_t,\quad Z=0\\ B_e\cdot\theta_e^a & R_t<R<1,\quad Z=0\end{cases}$$

$$\frac{\partial\theta(R,Z)}{\partial Z}+B_i\cdot\theta(R,Z)=0 \qquad 0<R<1,\quad Z=Z_{max}$$

$$\frac{\partial\theta(R,Z)}{\partial R}=0 \qquad R=0 \text{ or } 1,\quad 0<Z<Z_{max} \tag{1}$$

In these equations, the dimensionless and reduced variables are defined by

$$R=\frac{r}{r_w} \qquad R_t=\frac{r_t}{r_w}$$

$$Z=\frac{z}{r_w} \qquad Z_{max}=\frac{z_{max}}{r_w}$$

$$B_e=H_e\frac{r_w}{k} \qquad B_i=H_i\frac{r_w}{k}$$

$$\theta=T-T_i^a \qquad \theta_e^a=T_e^a-T_i^a$$

$$D=\alpha_t r_w(I_c+I_d)/k \qquad G=\frac{r_w}{k}\frac{\partial Q}{\partial Z} \tag{2}$$

Q is the radiative flux inside the medium and the term G contains it divergence. The distributions of Q and G depend

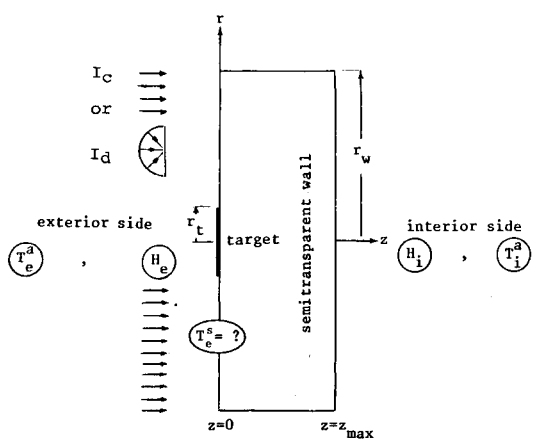

Fig. 1 Problem representation.

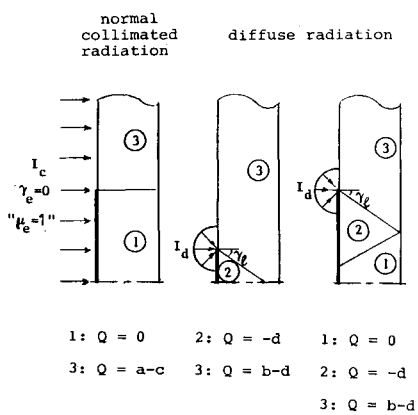

Fig. 2 Different zones created by the target radius and the nature of radiation falling from outside.

on the nature of the external radiation, on the opaque target size, and on the position inside the medium. This is illustrated in Fig. 2. A general treatment of this problem would obviously require the evaluation of $Q = Q(R, Z)$ and $G = G(R, Z)$.

A simplified treatment was carried out here, leading to expressions for Q independent of R. It is based on a separate evaluation of the radiative transfer equation in nonshadowed and shadowed zones, supposed without mutual radiative interaction.

For the nonshadowed zones of the layer, the radiative flux is given by the following equations[4-6]:

$$Q(Z) = Q^+(Z) - Q^-(Z)$$

$$Q^+(Z) = \underbrace{\mu_e I_c \sum_{n=1}^{N} \frac{F_n}{\psi_n} \tau_n \exp\left(-\kappa_n \frac{Z}{\mu}\right)}_{\text{a}} + \underbrace{2I_d \sum_{n=1}^{N} F_n \phi_3(\tau_n, \kappa_n Z)}_{\text{b}}$$

$$Q^-(Z) = \underbrace{\mu_e I_c \sum_{n=1}^{N} \frac{F_n}{\psi_n} \tau_n \exp\left(-\kappa_n \frac{Z}{\mu}\right) \rho_n \exp\left(-\kappa \frac{2Z_{\max} - Z}{\mu}\right)}_{\text{c}}$$

$$+ \underbrace{2I_d \sum_{n=1}^{N} F_n \phi_3[\tau_n \cdot \rho_n, \kappa_n(2Z_{\max} - Z)]}_{\text{d}} \tag{3}$$

where

$$\mu = \cos \gamma$$

$$\psi_n(\mu) = 1 - \rho_n^2 \exp\left(-2\kappa_n \frac{Z_{\max}}{\mu}\right)$$

$$\phi_3(a, b) = \int_{\mu_l}^{1} \frac{a \exp(b/\mu)\mu}{\psi_n(\mu)} \, d\mu \tag{4}$$

F_n is the blackbody emissive power fraction within the nth wavelength interval $\lambda \in (\lambda_{n-1/2}, \lambda_{n+1/2})$ for a given source temperature. The term μ is calculated from μ_e, the value corresponding to the external incidence angle of radiation γ_e, using Snell's law with the spectral refractive indexes of both medium and surroundings being known.

The lower limit of integration μ_l in Eq. (4) corresponds to the limit angle γ_l bounding the transmitted intensities incident from outside. Its value depends on the wavelength through the refractive index, which makes the problem more complicated. Fortunately, the variation of the refractive index with the wavelength can be neglected for the media and wavelength range considered here. The spectral surface reflectivities ρ_n and, hence, transmittivities τ_n are calculated from Fresnel's law.

For the shadowed zones of the slab, Q is computed accounting for the contributions of different terms (noted a–d) of Eqs. (3) (see Fig. 2). In order to simplify the analysis and to preserve the axisymmetry of the radiative field, only normal incidence is considered for the collimated component.

Equations (3) and (4), through integration over the appropriate solid angle, account for the directional effects of radiation near the opaque disk. Another simplification introduced in the model is to neglect, in the term D representing the boundary condition on the opaque disk [expressions (2)], the contribution of the absorbed radiation coming from within the semitransparent material. Since the collimated radiation is supposed normal, this contribution is limited to the diffuse component reflected back to the opaque disk by the back face of the slab. Owing to the order of magnitude of the refractive index of Plexiglas and borosilicate glass (<1.5), the angle of incidence of radiation onto the back surface of the slab is less than 41.8 deg. The corresponding reflectivities of the interfaces are less than 0.05. This allows to neglect the radiative flux reflected by the back surface of the slab and absorbed by the backside of the opaque disk.

The conduction problem with source term can be solved analytically using the method of separation of variables associated with the integral transform technique.[7,8] The main features of the solution are presented in the Appendix.

A simpler numerical finite-difference solution is also given by Roissac.[9] However, the analytical solution is easy to program, in spite of its apparent complexity. It allows the computation of the temperature directly and independently at any point in the specified domain.

The correction term ΔT, i.e., the amount of temperature perturbation caused by the target, may be estimated by the difference between the temperature $T(R, Z)$ calculated at a nonperturbed surface point [$T(1, 0)$ far from the target, in practice, a distance greater than two times the target diameter is large enough] using Eq. (A19), and the temperature calculated at the measurement point [$T(0, 0)$ i.e., at the target center] using the same equation. Due to the simplifications introduced in the model, these two calculated temperatures $T(1, 0)$ and $T(0, 0)$, do not correspond to exact values. However, their difference ΔT well approaches the real perturbation.

The term ΔT is a function of many parameters, including 1) r_t, 2) α_t, 3) the difference between the two ambient temperatures $\theta_e^a = T_e^a - T_i^a$, 4) the heat transfer coefficients H_e and H_i, 5) the physical properties characterizing the semitransparent material, and 6) the incident radiation intensity I. The nature of the incident radiation (e.g., diffuse or normally collimated) has nearly no effect on ΔT. This was shown from a numerical simulation by Roissac.[9]

In order to examine the influence of the above parameters, a theoretical parametric study is first carried out on a Plexiglas specimen. The advantage of choosing this material is that it is relatively easy, for experimental purposes, to embed thermocouples.

The spectral refractive index and absorptivity used in the computations are those given by Lumsdaine,[10] and the thermal conductivity is that estimated at room temperature by Raynaud[11] ($k = 0.198$ W·m^{-1}·°C^{-1}).

Figure 3 shows the computed temperature field for the parameters specified on the figure, which correspond to a moderate incident radiation and a black spot of radius r_t = 50 mm. The amplitude of the front surface temperature variation is 11.2°C. It can be seen that the temperature perturbation extends over an area of radius equal to about two times the target radius. The amplitude of perturbation decreases with the depth inside the slab.

Figure 4 shows for the same conditions, but with variable r_t, the influence of the spot size on the front surface temperature field. Even under these moderate conditions, decreasing

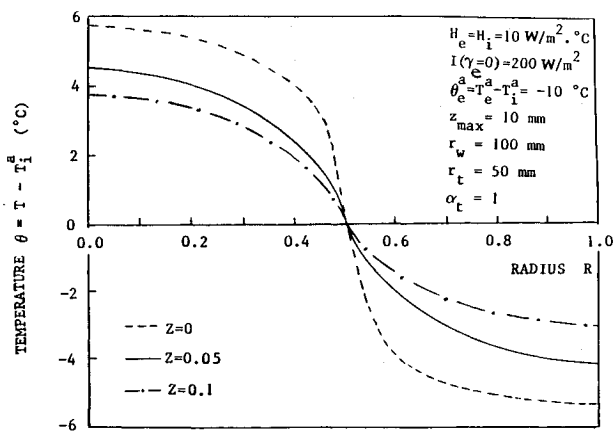

Fig. 3 Temperature field in the Plexiglas wall. Case of normal collimated irradiation.

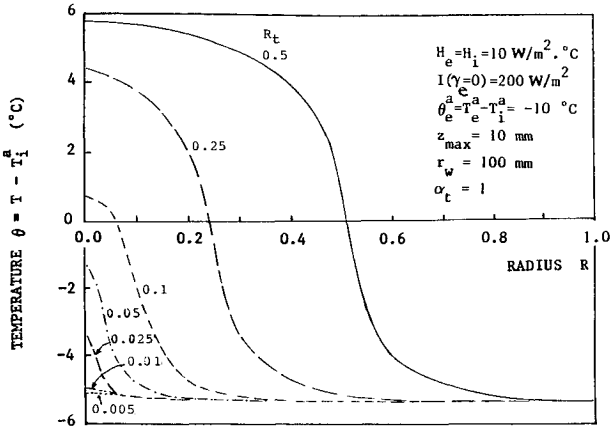

Fig. 4 Influence of target size on the surface temperature. Case of normal collimated irradiation.

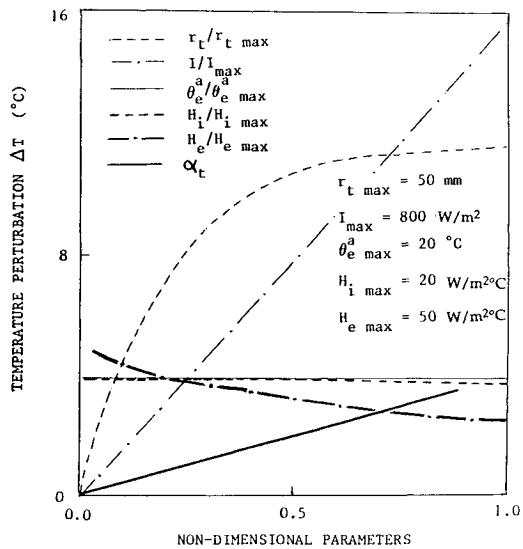

Fig. 5 Effect of nondimensional parameters on ΔT.

the spot radius down to r_t = 5 mm, gives a temperature variation of amplitude 3.91°C. Starting from the following set of data:

$$\begin{aligned} r_t &= 5 \text{ mm} \\ H_e &= 10 \text{ W}\cdot\text{m}^{-2}\cdot{}^\circ\text{C}^{-1} \\ T_e^a - T_i^a &= -10^\circ\text{C} \\ \alpha_t &= 1 \\ H_i &= 10 \text{ W}\cdot\text{m}^{-2}\cdot{}^\circ\text{C}^{-1} \\ I_c &= 200 \text{ W}\cdot\text{m}^{-2} \end{aligned}$$

used as a basic case, by changing individually the value of each parameter, one can examine its effect on ΔT. Figure 5 shows the variation of ΔT with these parameters in a nondimensional form. It can be seen that ΔT 1) increases with the increase in α_t, r_t, and I_c; 2) decreases with the increase in H_e; and 3) remains nearly constant for variables H_i and θ_e^a.

A similar study is carried out using a borosilicate glass specimen of thermal conductivity k = 1 W·m^{-1}·°C^{-1}, and spectral thermo-optical properties given by Kunc.[12] Similar results are obtained and compared to those of the Plexiglas specimen, as shown on Fig. 6.

According to this theoretical study, a target of small radius and low absorptivity may be used to decrease ΔT. This result could have been anticipated. However, the selection of the target radius depends on the optical performance of the radiometer, which should be appropriately chosen. On the other hand, a low absorptivity means a high reflectivity. Therefore, in a practical application, a part of the externally falling ra-

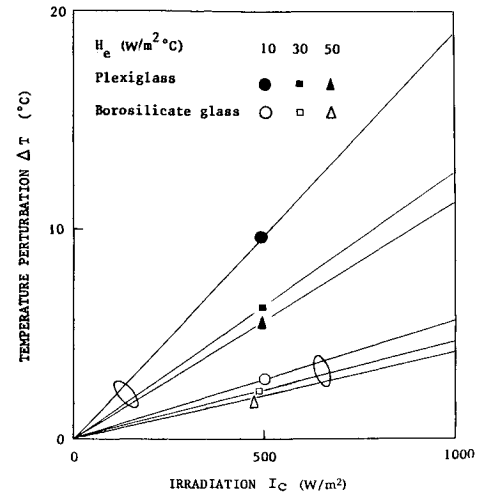

Fig. 6 Effect of I and H_e on ΔT for different materials.

diation is reflected by the target back to the radiometer. This reflected radiation is a parasite which leads to erroneous target temperature measurement. Therefore, a compromise is necessary according to the objective. We are particularly interested in a correct surface temperature, not especially in a low ΔT. The correct surface temperature is obtained from

$$T^s_{\text{corrected}} = T^s_{\text{measured}} + \Delta T$$

where T^s_{measured} is the surface temperature measured at the target center by means of a good quality pyrometer (that is capable of providing accurate measurements on small targets near room temperature).

Provided that ΔT is sufficiently correct, the value of T^s_{measured} should be as correct as possible to get a good $T^s_{\text{corrected}}$. A good T^s_{measured} is obtainable only if the target is of high absorptivity. The choice of a high absorptivity target is essential. In addition, if a small ΔT is also sought, one can use a small size target.

Surface Reference Temperature Calculation (T^s_{ref})

We present here the model used to determine the specimen surface temperature from measurements carried out using two embedded thermocouples.

The surface temperature is obtained by solving the following inverse problem:

$$\frac{\mathrm{d}}{\mathrm{d}z}\left[-k\frac{\mathrm{d}T(z)}{\mathrm{d}z} + Q(z)\right] = 0 \qquad 0 < z < z_{\max}$$

$$T(z) = T^s_e = T^s_{\text{ref}} \quad \text{(unknown)} \qquad z = 0$$

$$T(z) = T^s_i \quad \text{(unknown)} \qquad z = z_{\max}$$

The temperature should be known at two locations inside the specimen. k is also assumed known. The term $Q(Z)$ is given by Eq. (3). For limited temperature ranges, where k may be considered constant, the solution becomes

$$T(z) = T^s_e - \frac{z}{z_{\max}}\left[T^s_e - T^s_i + \frac{1}{k}\int_0^{z_{\max}} Q(z)\,\mathrm{d}z\right] + \frac{1}{k}\int_0^z Q(z')\,\mathrm{d}z'$$

T^s_e and T^s_i are unknown, but using temperature measurements at two different positions $z1$ and $z2$ inside the specimen,

we get the following equations:

$$\left(1 - \frac{z1}{z_{max}}\right) T_e^s + \left(\frac{z1}{z_{max}}\right) T_i^s = T_{z1} - \frac{1}{k}\int_0^{z1} Q(z)\,dz + \frac{z1}{z_{max}k}\int_0^{z_{max}} Q(z)\,dz$$

$$\left(1 - \frac{z2}{z_{max}}\right) T_e^s + \left(\frac{z2}{z_{max}}\right) T_i^s = T_{z2} - \frac{1}{k}\int_0^{z2} Q(z)\,dz + \frac{z2}{z_{max}k}\int_0^{z_{max}} Q(z)\,dz$$

from which T_e^s and T_i^s are obtained.

The temperatures T_{z1} and T_{z2} inside the specimen are accurately measured using carefully calibrated thermocouples. This procedure leads to accurate values of T_e^s (accuracy better than 0.1°C) which will be used as reference temperatures to validate the radiometric technique.

The effect of thermocouples on the temperature field should be examined separately. The opaque, and supposedly gray, thermocouple wire of surface area A and absorptivity α_c is considered to absorb the radiation according to the relation

$$Q_{abs} \approx Q(z) \cdot \alpha_c \cdot A$$

where Q_{abs} is the absorbed radiation, and $z = z1$ or $z2$ is the thermocouple position. Clearly, the thermocouples effect becomes less important for low Q_{abs}, and hence, for low $Q(z)$, α_c, and A values. This has been confirmed quantitatively through a simple finite-difference model proposed by Roissac.[9] The absorbed energy is assumed to be rediffused in the medium, by conduction, with the thermocouples considered as cylindrical heat sources. It is shown that the effect of thermocouples, represented by the maximum temperature rise in the medium, is very weak, even with $\alpha_c = 1$. For experimental conditions similar to those used in the present study, the effect of thermocouples can be neglected.

Experimental Setup and Data

Experiments were carried out in a controlled cell and in a natural ambiance. In either case, the surface temperature of a semitransparent specimen was estimated under different conditions in two ways: 1) through radiometric measurements carried out on small opaque targets of known absorptivities and perfectly glued to the specimen surface (this temperature will be corrected using the technique just presented to get the true temperature $T^s_{corrected}$); and 2) by using internal temperature measurements carried out by means of two thermocouples embedded in a nonperturbed region, to get the reference temperature T^s_{ref}. Figure 7 shows the locations of these thermocouples inside the specimen. In fact, three thermocouples were used in order to try different combinations of two measurements.

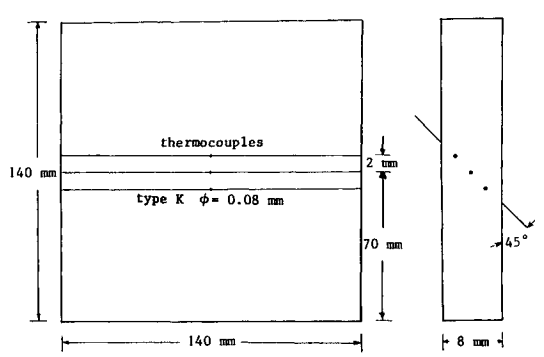

Fig. 7 Plexiglas specimen.

Comparisons are carried out between $T^s_{corrected}$ and T^s_{ref} to evaluate the pyrometer technique, and to give the best operating conditions.

Several small-size targets are placed sufficiently far from each other on the surface. The spectral quasinormal emissivities of these targets—necessary to compute the correction term ΔT—were previously measured using a parabolic reflectometer.[13] This setup allows the measurement of the spectral radiation reflected by the target, then by a reference surface, at each incidence angle. Their ratio leads to the target reflectivity, and hence, to its emissivity. The results are shown in Fig. 8. On the other hand, the mean emissivity of each target in the pyrometer spectral band (8–14 μm)—necessary to carry out the radiometric measurements—are obtained using a direct method.[9] In this method, the pyrometer is used to sight successively the concerned target and a blackbody at the same temperature to get the required emissivities, as shown on Table 1. The measured emissivity values are nearly constant in the temperature range of the experiments. The spectral thermophysical properties of the Plexiglas are given by Lumsdaine.[10] The incident radiation intensity is measured by a photovoltaic cell, calibrated using a Kipp and Zonen pir-anometer, and placed on the irradiated specimen's surface. Finally, noting that H_i has a negligible effect on ΔT, one can consider that $H_i \approx H_e$. An iterative procedure may be needed to estimate H_e, which is function of the surface mean temperature.

Table 1 Mean emissivities of different targets, λ = 8–14 μm

Target nature	Emissivity
3M 2010 Black Velvet paint	0.95
Black Mecanorma labels	0.92
Aerosol white paint	0.90
Aerosol metallic paint	0.60

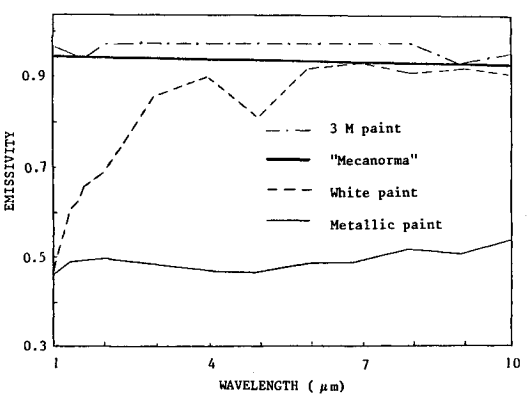

Fig. 8 Spectral emissivities of different targets.

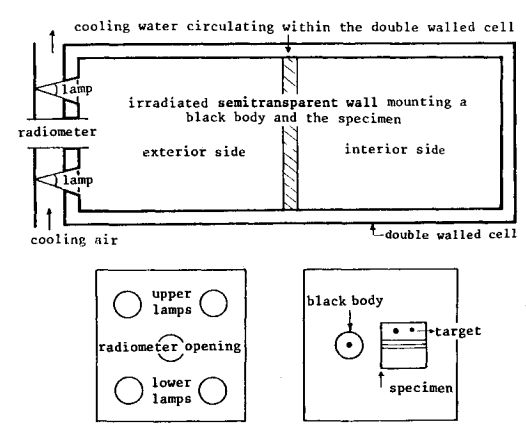

Fig. 9 Controlled cell setup.

The controlled cell setup is shown on Fig. 9. It includes two compartments simulating the external and the internal ambiances. The internal surfaces of the cell are painted black to reduce the reflected radiation. The temperature of these surfaces is regulated by circulating water of controlled temperature within the double walls of the cell. The two compartments are separated by a Plexiglas plate of the same thickness as the sample, on which are mounted the specimen and a blackbody, which is used to calibrate the radiometer. The external side of the plate is rather uniformly irradiated by four lamps appearing from windows in front of it. A reasonable uniformity and diffuseness of the semitransparent wall irradiation in the region of the sample was checked by means of a small radiation cell moved and rotated close to the sample. The lamps are cooled by air ventilation to reduce the infrared radiation. The radiometer can sight the targets and can be calibrated on the blackbody through a fifth central window, as those of the lamps. The ambient temperature in each compartment is measured by thermocouples stretched parallel to the Plexiglas plate and well screened from radiation.

The outdoor setup is composed of the Plexiglas plate on which are mounted the specimen and a solarimeter. The plate can be oriented with respect to the sun by means of a simple mechanical system. The setup also involves an anemometer to measure the wind speed, and a piranometer to measure the solar irradiation.

The values of H_e and H_i needed to evaluate the correction term ΔT are obtained through the following relation, taking into account the radiative and convective exchanges of the sample surface with its surroundings of ambient temperature T^a:

$$H = C[(T^s - T^a)/L]^{1/4} + 4\sigma\varepsilon[(T^s + T^a)/2]^3$$

where C is a coefficient depending on the type of convection and plate position (1.42 for natural laminar convection of air on a vertical plate) and L is the plate length. The second term of this expression accounts for the IR radiative exchanges of the plate surface with the surroundings, in the opacity wavelength range of the material. In a practical situation where the surface temperature is not known, an iterative procedure is used with an initial value for the mean surface temperature T^s equal, for instance, to that measured at the target center T^s_{measured}. Having calculated H_e and $H_i \approx H_e$, one can determine ΔT, from which a new value for T^s is obtained, through the relation

$$T^s = T^s_{\text{measured}} + \Delta T$$

The procedure continues until a convergence criteria is satisfied.

Results and Discussion

Table 2 shows the specimen exterior and interior surface temperatures T^s_i and T^s_e extrapolated through the measurements, carried out by three combinations of two embedded thermocouples each.

The combination of thermocouples placed near the surfaces lead to values for T^s_i and T^s_e ($=T^s_{\text{ref}}$) lying between those obtained from the other two combinations. This combination was adopted to give the reference temperature T^s_{ref}.

Tables 3 and 4 show some results obtained from the controlled cell and the outdoor experiments, respectively. The comparison of $T^s_{\text{corrected}}$ and T^s_{ref} shows excellent agreement between them, which means that the correction ΔT is reasonably accurate. Although higher perturbation ΔT are created by the black targets, less errors $|T^s_{\text{corrected}} - T^s_{\text{ref}}|$ are introduced when using them. The reason is not difficult to find: for $I \neq 0$, a higher absorptivity leads to a higher target temperature, and therefore, to a higher ΔT, as already shown on Fig. 5. On the other hand, and due to the corresponding low target reflectivity, less radiation is reflected toward the pyrometer sighting the target. This leads to more accurate

Table 2 Extrapolated surface temperatures using three combinations of two thermocouples each

T Measured using two thermocouples			T Extrapolated with $I = I_c = 210$ W/m²		T Extrapolated with $I = I_d = 210$ W/m²	
T_{z1}	T_{z2}	T_{z3}	$T^s_{\text{ref}(T^s_e)}$	T^s_i	$T^s_{\text{ref}(T^s_e)}$	T^s_i
14.80	15.55		14.646	16.126	14.644	16.119
	15.55	15.91	14.913	15.929	14.995	15.928
14.80		15.91	14.666	15.934	14.664	15.934

Table 3 Results obtained from the controlled cell experiments

Surrounding conditions with $H_e = H_i = 10$ W/m²°C						
I_d, W/m²	0	0	56	56	210	210
T^a_e, °C	10.9	28.2	11.7	30	13.9	31.4
T^a_i, °C	19.9	22.8	20.4	23.3	22.0	24.7
3M Target of $\phi = 10$ mm						
T^s_{measured}, °C	15.1	26.2	17.0	28.6	24.2	35.7
ΔT, °C	0.0	0.0	−0.9	−1.0	−3.6	−3.6
$T^s_{\text{corrected}}$, °C	15.1	26.2	16.1	27.6	20.6	32.1
White target of $\phi = 10$ mm						
T^s_{measured}, °C	13.8	27.2	15.4	28.3	21.7	34.5
ΔT, °C	0.0	0.0	−0.7	−0.7	−3.5	−3.5
$T^s_{\text{corrected}}$, °C	13.8	27.2	14.7	27.6	18.2	31.0
Metallic target of $\phi = 10$ mm						
T^s_{measured}, °C	11.5	28	14.8	30.6	21.4	36.9
ΔT, °C	0.0	0.0	−0.5	−0.5	−1.8	−1.8
$T^s_{\text{corrected}}$, °C	11.5	28	14.3	30.1	19.6	35.1
Black Mecanorma target of $\phi = 10$ mm						
T^s_{measured}, °C	14.7	26	16.9	28.5	24.2	35.4
ΔT, °C	0.0	0.0	−0.9	−0.9	−3.5	−3.5
$T^s_{\text{corrected}}$, °C	14.7	26	16	27.6	20.7	31.9
Black Mecanorma target of $\phi = 7$ mm						
T^s_{measured}, °C	14.7	26	16.7	28.4	23.8	35.1
ΔT, °C	0.0	0.0	−0.8	−0.8	−3	−3
$T^s_{\text{corrected}}$, °C	14.7	26	15.9	27.6	20.8	32.1
Reference surface temperature (extrapolated)						
T^s_{ref}, °C	14.9	26.3	15.8	28.1	20.4	32.2

Table 4 Results obtained from outdoor experiments using black Mecanorma targets

Pyrometer type target, diameter mm	KT4S 10		CYCLOP 33 20		UX 41 20	
I_c, W/m²	761	804	421	705	763	786
T^s_{measured}, °C	43	45.1	41	55	54.4	51.2
ΔT, °C	−12.3	−13.4	−12	−20.1	−21.7	−22.4
$T^s_{\text{corrected}}$, °C	30.7	31.7	29	34.9	32.7	28.8
T^s_{ref}, °C	29.3	30.4	27.9	34.3	34.8	29.7

target temperature measurement $T^s_{measured}$, i.e., to more precise corrected surface temperature ($T^s_{corrected} = T^s_{measured} + \Delta T$), and hence, to less deviation from the reference surface temperature T^s_{ref}. As we pointed out, ΔT is sufficiently accurate regardless of its value (low or high). However, it can be reduced by using small radius targets. This was shown on Fig. 5 and is confirmed here for the black "Mecanorma" targets. One can conclude that the use of small black targets represents a good compromise. Finally it should be pointed out that the outdoor experiments were carried out under uncontrolled conditions for which steady state was barely obtained. Even though, the maximum error $|T^s_{corrected} - T^s_{measured}|$ is less than 2.5°C, i.e., less than 7%. These results confirm the interest of this technique.

Conclusions

An efficient method to measure the surface temperature of a semitransparent wall, placed in a convective medium at moderate temperatures and exposed to external radiation like solar radiation, is given in this article. In this method, radiometric measurement is carried out on a black small size and very thin adhesive target of known spectral radiative properties, perfectly adhered to the concerned surface. The true surface temperature can be obtained by adding a correction term to the target temperature, measured by the pyrometer. The correction term is obtained through a model, elaborated to solve a coupled conduction-radiation heat transfer problem in a "cold medium" of known spectral thermo-optical properties.

Several experiments were designed to apply this method under different conditions. The corrected surface temperature measurements were compared to exact reference surface temperature so as to validate the proposed technique. The reference temperatures were obtained through the solution of an inverse heat transfer problem in a nonperturbed area of the semitransparent wall (far from the target position). The inverse solution is based on temperature measurements carried out inside the specimen, using embedded thermocouples, and then extrapolated to yield the surface temperature.

Sufficiently accurate results can be achieved along with the use of black targets. Low perturbation level can be attained by decreasing the target diameter. The target may be a simple adhesive black label, commercially available in a wide diameter range. The method is simple, flexible, and can be successfully applied even under less controlled conditions with the steady-state situation hardly maintained.

For building glass windows temperature measurement, this method avoids the problems associated with the use of contact sensors (thermal resistance of contact, fragility, inaccuracy, etc.). It necessitates a metrological package comprising an accurate IR pyrometer and some simple devices to estimate the ambient conditions and solar irradiation. A data bank of correction term calculated from the model for the most commonly used materials, need build-up. Then the correction term can be obtained graphically or directly using a dedicated calculator.

Appendix: Analytical Solution of the Conduction Problem

Taking the integral transform of the governing Eqs. (1) with respect to the space variable R yields

$$-\beta_m^2\tilde{\theta}(\beta_m, Z) + \frac{d^2\tilde{\theta}(\beta_m, Z)}{dZ^2} + \tilde{G}(\beta_m, Z) = 0$$

$$0 < Z < Z_{max}$$

$$-\frac{d\tilde{\theta}(\beta_m, Z)}{dZ} + B_e\tilde{\theta}(\beta_m, Z) = \tilde{E}(\beta_m) \qquad Z = 0$$

$$\frac{d\tilde{\theta}(\beta_m, Z)}{dZ} + B_i\tilde{\theta}(\beta_m, Z) = 0 \qquad Z = Z_{max} \qquad \text{(A1)}$$

where β_m are the eigenvalues satisfying the equation $J_1(\beta_m) = 0$ which involves the Bessel function of first kind of order 1.

$\tilde{\theta}$, $\tilde{E}$, and $\tilde{G}$ are the integral transforms of θ, B_e, θ_e^a (or $B_e\theta_e^a + D$, following the values of R) and G, respectively. Specifically θ is defined by

$$\tilde{\theta}(\beta_m, Z) = \int_0^1 R\cdot J_0(\beta_m R)\cdot\theta(R, Z)\, dR \qquad \text{(A2)}$$

where J_0 is the Bessel function of first kind of order zero. It can be shown that

$$\tilde{E}(\beta_m) = (B_e\theta_e^a + D)\int_0^{R_t} R\cdot J_0(\beta_m R) + B_e\theta_e^a \times \int_{R_t}^1 R\cdot J_0(\beta_m R)\, dR = \frac{1}{\beta_m}[D\cdot R_t\cdot J_1(\beta_m R_t)] \qquad \text{(A3)}$$

$$\tilde{G}(\beta_m, Z) = \int_0^1 R\cdot J_0(\beta_m R)\cdot G(Z)\, dR = \sum_{p=1}^{M-1} G_p(Z)\int_{R_p}^{R_{p+1}} R\cdot J_0(\beta_m R)\, dR = \frac{1}{\beta_m}\sum_{p=1}^{M-1} G_p(Z)[R_{p+1}\cdot J_1(\beta_m R_{p+1}) - R_p\cdot J_1(\beta_m R_p)] \qquad \text{(A4)}$$

where M is the number of different irradiation zones created inside the wall by the presence of the target and the irradiation type.

For $\beta_m = 0$, the values of $\tilde{E}$ and $\tilde{G}$ may be obtained while making use of the relation[7]

$$\lim_{\beta\to 0}[J_1(\beta_m R)/\beta_m] = (R/2) \qquad \text{(A5)}$$

In this case

$$\tilde{E}(0) = (DR_t^2/2) \qquad \text{(A6)}$$

$$\tilde{G}(0, Z) = \frac{1}{2}\sum_{p=1}^{M-1} Gp(Z)[R_{p+1}^2 - R_p^2] \qquad \text{(A7)}$$

The solution of system [Eq. (A1)] for $\beta_m = 0$ may be expressed as[9]

$$\tilde{\theta}(0, Z) = \int\left[\int \tilde{G}(0, Z)\, dZ\right] dZ + C1\cdot Z + C2 \qquad \text{(A8)}$$

where $C1$ and $C2$ are the integration constants

$$C1 = -\frac{r_w}{k}\left[\int_0^{z_{max}} \tilde{Q}(0, Z)\, dZ + \frac{1}{B_i}\tilde{Q}(0, Z_{max}) + \frac{1}{B_e}\tilde{Q}(0, 0)\right]\left(\frac{1}{B_i} + \frac{1}{B_e} + Z_{max}\right)^{-1} \qquad \text{(A9)}$$

$$C2 = \left\{\left(Z_{max} + \frac{1}{B_i}\right)\left[\tilde{E}(0) + \frac{r_w}{k}\tilde{Q}(0, 0) - \frac{r_w}{k}B_e \times \int \tilde{Q}(0, Z)\, dZ|_{Z=0}\right] - \frac{r_w}{k}\left[\int \tilde{Q}(0, Z)\, dZ|_{Z=Z_{max}} + \frac{1}{B_i}\tilde{Q}(0, Z_{max})\right]\right\}\left[B_e\left(\frac{1}{B_i} + \frac{1}{B_e} + Z_{max}\right)\right]^{-1} \qquad \text{(A10)}$$

$$\tilde{Q}(0, Z) = \frac{1}{2}\sum_{p=1}^{M-1} Q_p(Z)(R_{p+1}^2 - R_p^2) \qquad \text{(A11)}$$

as for $\tilde{G}$ with $\beta_m = 0$

For $\beta_m \neq 0$, the solution of the same system would be[9]

$$\tilde{\theta}(\beta_m, Z) = C3\cdot e^{\beta_m Z} + C4\cdot e^{-\beta_m Z} + \frac{1}{\beta_m} \times \int \tilde{G}(\beta_m Z')\sinh[\beta_m(Z - Z')]\, dZ' \qquad \text{(A12)}$$

where $C3$ and $C4$ are obtained by applying the boundary conditions of the system [Eq. (A1)]

$$C3 = [U(\beta_m - B_i)\exp(-\beta_m Z_{\max}) - V(\beta_m + B_e)]/Y \qquad \text{(A13)}$$

$$C4 = [U(\beta_m + B_i)\exp(-\beta_m Z_{\max}) - V(\beta_m - B_e)]/Y \qquad \text{(A14)}$$

$$U = \tilde{E}(\beta_m, 0) - \frac{B_e}{\beta_m}\int \tilde{G}(\beta_m, Z')\sinh[\beta_m(Z - Z')]\, dZ|_{Z=0} + \frac{1}{\beta_m}\frac{d}{dZ}\int \tilde{G}(\beta_m, Z')\sinh[\beta_m(Z - Z')]\, dZ|_{Z=0} \qquad \text{(A15)}$$

$$V = \frac{B_i}{\beta_m}\int \tilde{G}(\beta_m, Z')\sinh[\beta_m(Z - Z')]\, dZ|_{Z=Z_{\max}} + \frac{1}{\beta_m}\frac{d}{dZ}\int \tilde{G}(\beta_m, Z')\sinh[\beta_m(Z - Z')]\, dZ|_{Z=Z_{\max}} \qquad \text{(A16)}$$

$$Y = 2[(\beta_m^2 + B_i B_e)\sinh(\beta_m Z_{\max}) + \beta_m(B_i + B_e)\cosh(\beta_m Z_{\max})] \qquad \text{(A17)}$$

The solution $\theta(R, Z)$, and therefore, the amount of perturbation ΔT, can be obtained by introducing $\theta(\beta_m, Z)$ in the following inversion formula[7,9]:

$$\theta(R, Z) = 2\sum_{m=1}^{\infty}\frac{J_0(\beta_m R)}{J_0^2(\beta_m)}\cdot\tilde{\theta}(\beta_m, Z) \qquad \text{(A18)}$$

to get

$$\theta(R, Z) = 2\int\int \tilde{G}(0, Z')\, dZ'\, dZ'' + C1\cdot Z + C2 + 2\sum_{m=0}^{\infty}\frac{J_0(\beta_m R)}{J_0^2(\beta_m)}\left\{C3\cdot e^{\beta_m Z} + C4\cdot e^{-\beta_m Z} + \frac{1}{\beta_m}\int \tilde{G}(\beta_m, Z')\sinh[\beta_m(Z - Z')]\, dZ'\right\} \qquad \text{(A19)}$$

References

[1]Werling, E., "Contribution aux Mesures par Contact de Températures de Surface de Parois Semi-Transparentes, Modélisation—Expérimentation," Thèse, No. ordre: 87 ISAL 0054, INSA, Lyon, France, 1988.

[2]Pauzin, S., "Contribution à l'Etude du Transfert Radiatif en Milieu Diffusant," Thèse, Université Pierre et Marie Curie, Paris, France, 1981.

[3]Chupp, R. E., and Viskanta, R., "Development and Evaluation of a Remote Sensing Technique for Determining the Temperature Distribution in Semi-Transparent Solids," *Journal of Heat Transfer*, Vol. 96, No. 3, 1974, pp. 391–397.

[4]Siegel, R., and Howell, J. R., *Thermal Radiation Heat Transfer*, Hemisphere, Washington, DC, 1981.

[5]Viskanta, R., and Anderson, E. E., "Heat Transfer in Semi-Transparent Solids," *Advances in Heat Transfer*, Vol. 11, Academic Press, New York, 1975, pp. 317–441.

[6]Viskanta, R., and Hirleman, E. D., "Combined Conduction-Radition Heat Transfer Through an Irradiated Semi-Transparent Plate," *Journal of Heat Transfer*, Vol. 100, No. 1, 1978, pp. 169–172.

[7]Ozisik, M. N., *Heat Conduction*, Wiley, New York, 1980.

[8]Carslaw, H. S., and Jaeger, J. C., *Conduction of Heat in Solids*, 2nd ed., Oxford Univ. Press, Oxford, England, UK, 1959.

[9]Roissac, F. Z., "Modélisation et Etude Expérimentale du Transfert de Chaleur par Rayonnement et Conduction Couplés dans un Milieu Semi-Transparent soumis à des Conditions aux Limites Non Uniformes," Thèse, INSA, Lyon, France, 1989.

[10]Lumsdaine, E., "Solar Heating of a Fluid Through a Semi-Transparent Plate: Theory and Experiment," *Solar Energy*, Vol. 12, No. 6, 1968, pp. 457–467.

[11]Raynaud, M., "Détermination du Flux Surfacique Traversant une Paroi à Partir de Mesures de Température Internes," Thèse, Université Pierre et Marie Curie, Paris, France, 1984.

[12]Kung, T., Lallemand, M., and Saulnier, J. B., "Some New Developments on Coupled Radiative-Conductive Heat Transfer in Glasses: Experiments and Modelling," *International Journal of Heat and Mass Transfer*, Vol. 27, No. 12, 1984, pp. 2307–2319.

[13]Al Hamwi, M., "Mesure de la Réflectivité Spectrale Directionnelle de Matériaux Opaques Métalliques et Non Métalliques: Mise au Point d'un Réflectomètre à Miroirs Paraboliques," Thèse, No. ordre: IDI 19001, INSA, Lyon, France, 1990.